XLI CILAMCE
XLI Ibero-Latin American Congress on Computational Methods in Engineering
16-19 November, 2020 FOZ DO IGUAÇU PARANÁ - BRAZIL

# Theoretical-Experimental Analysis of Corrosion-Cracking Coupling in Reinforced Concrete Structures

Samanta A. Klering[1a], Thiago A. Bertuzzo[1b], Edna Possan[1c], Julio Flórez-López[1d]

[1]*Latin American Institute of Technology, Infrastructure and Territory, Federal University of Latin American Integration. Foz do Iguaçu, Paraná, Brazil*
[a] *samaandri@hotmail.com,* [b] *thiagobertuzzo@gmail.com,* [c] *epossan@gmail.com, j.* [d] *florezlopez@gmail.com*

**Abstract.** The corrosive process is not a recent problem, however, even nowadays it is one of the most common problems on reinforced concrete structures, whether by execution inconveniences, by the high relation water/cement of concrete or even by the negligence in the project stage of consideration of an adequate covering which attends the corresponding aggressiveness of the class. Therefore, the previous determination of the evolution of the corrosion along time shows itself as an allied tool in the reduction of costs with maintenance and/or repairs. In this context, the following paper aimed to identify experimentally, in beams, the influence of the corrosion evolution by chloride ions in the advance of degradation from the elements of reinforced concrete. A process of acceleration of the corrosion was used through the sprinkling of a sodium chloride solution (NaCl) via a sprayer, simulating the effect of wetting/drying in the breams. Simultaneously, the beams were under mechanic solicitations, so as the experiment advanced the deflections, cracking and especially the corrosion potential in the rebars were evaluated. Later, after this identification, the experimental analysis was combined with thermodynamic models based on the Lumped Damage Mechanics to analyze reinforced concrete structures that are subject to chemical action in addition to mechanical stresses. It was found that all beams subjected to the spraying of chlorides showed a greater than 90% probability of being under corrosion and the highest values of corrosion potential were concentrated in the central region of the beam, where the damage was also higher. Furthermore, the presence of corrosion increased the values of damage and plastic rotations in the beams, and this increase, in turn, contributed to the increase in corrosion rates. However, the presence of moisture due to the NaCl solution affected the creep and consequently, the displacements suffered over time.

**Keywords:** Reinforced Concrete, Damage Mechanics, Corrosion-Cracking Coupling.

## 1 Introduction

Concrete is used in almost all the ways of construction, even though, as Carvalho and Filho [1] describes that its use with no reinforce is not adequate, once the concrete shows high resistance to compression and low resistance when under traction. Therefore, the use of steel bars as a complement acting in order to reinforce and consequently improve the behavior of concrete under traction is a technique already accepted for years (KEARSLEY and JOYCE [2]).

Broomfield [3] quotes the economy and versatility of the use of reinforced concrete in construction, as due to the workability in the fresh state it is possible to have a variety of shapes and finishing. Besides allowing monolithic structures, given the existence of adherence between the concrete, which is put over the one already hardened, what does not happen in steel, wood or precast structures, for example. However, due to the big dimensions and high specific weight there are structures with large own weight (CARVALHO AND FILHO [1]).

Mostly, according to Broomfield [3], reinforced concrete is highlighted for its durability, resistance and a good performance along time. Yet, especially when the structure is exposed to aggressive environments, where the degradation usually escalates in a more accelerated rhythm, it is undeniable the possibility of deterioration of the element because of the corrosion (KIVELL, PALERMO and SCOTT [4]). Thus, it is justified the search for the creation of new project codes based on the performance, as emphasizes Kearsley and Joyce [2], who also affirm that it is necessary to take into consideration not only the time for the beginning of corrosion in the rebar, but also the estimation of necessary time for the evolution of the degradation reaches values in which the structure starts

not to correspond to its purpose.

According to Broomfiled [3], the problems caused by the corrosion in steel reinforcements are, nowadays, one of the most faced by civil engineers. Its most notorious effect is the reduction of the area of the transversal section of the bars affecting the resistance to bending. However, there are other related effects, for example, the accumulation of products of corrosion in the concrete/rebar interface which character is expansive and, therefore, may cause radial pressure in the concrete resulting in delamination and cracks (KIVELL, PALERMO and SCOTT [4]). In this paper, the evaluation is aimed in special to the loss of steel area.

In order to consider the effects of the action of corrosion studies as Coelho [5] and Dahmer [6] suggest methodologies based on the Lumped Damage Mechanics (LDM), which shows as an advantage the optimization computational for the analysis of structures of reinforced concrete, once to simplify it is considered that the cracks are concentrated in the plastic hinges (FLOREZ-LÓPEZ, MARANTE and PICÓN [7]). Dahmer [6] uses the Thermodynamics of Frames, besides LDM, where it is possible to verify the structure behavior through its useful life.

Notwithstanding, Brant [8] suggests a thermodynamically permissible model, where in addition to penalization due to the reduction of the steel area there is a consideration of the evolution of the process of cracking because of the rate of corrosion.

In light of this, the current study aims to verify the influence of corrosion evolution in the damage of a structural element of reinforced concrete, where it is expected that the same way the opening of crack causes the instauration of the damage process, it also provokes the evolution of the phenomenon of corrosion, which concomitantly influences the evolution of damage.

# 2 Numerical Model Including Damage, Plasticity and Corrosion

## 2.1 Thermodynamic Potential and Thermodynamic Forces Associated to the Internal Variables

The model used is capable to consider chemical phenomenon, once from the combination of Lumped Damage Mechanics with the tools of Thermodynamics of Frames, it begins to consider a new internal variable $c$ located in the extremities of the element, more specifically in the plastic hinges ($c_i$ e $c_j$), which shows the corrosion rate in the rebar existing in the structure and it is calculated by the eq. (1), where $\bar{p}$ is the average pit depth and $\phi$ is the original average diameter in the cross-section. In an illustrative way, the internal variables considered by the model (plastic rotations, damage and corrosion) are presented in Fig. 1.

$$c = cor = \frac{\bar{p}}{\bar{\phi}} \tag{1}$$

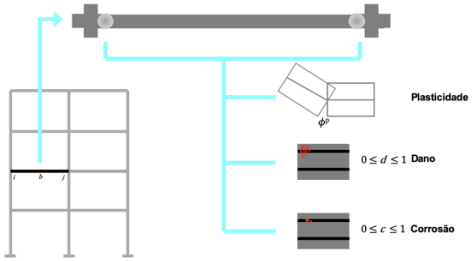


Figure 1. Internal variables located in the plastic hinges.

Due to the reduction in the transversal section of the steel bars caused by the corrosion, it is necessary to recalculate the steel area, since it affects the calculation of the initial properties of the section in the analysis. Therefore, the effective area is obtained by eq. (2) as suggested by Brant [8] based on Val and Melchers [9], in which $A_0$ corresponds to the initial steel area and $Kcor$ is defined by eq. (3).

$$A_{ef} = \frac{A_0}{\pi}\begin{cases} Kcor + \pi - arcsin2cor\sqrt{-cor^2+1}, & if\ cor < \dfrac{\sqrt{2}}{2} \\ Kcor + arcsin2cor\sqrt{-cor^2+1}, & if\ cor \ge \dfrac{\sqrt{2}}{2} \end{cases} \tag{2}$$

$$Kcor = -4cor^2 arcsin\sqrt{-cor^2+1} + 2cor\sqrt{-cor^2+1} \tag{3}$$

As mentioned previously, by the thermodynamic it is pursued to describe the problem through variables of state, which are derived from a potential to be defined. In this case, the potential written by Brant [8] which includes the damage, the plasticity and the corrosion is given by the eq. (4).

$$Gb_b = \frac{1}{2}\{\mathrm{M}\}^t[F(D)]\{\mathrm{M}\} + \{\mathrm{M}\}^t\{\Phi_0\} + \{\mathrm{M}\}^t\{\Phi^p\} - \frac{1}{2}\{\Phi^p\}^t[\mathrm{H(D,C)}]\{\Phi^p\} - I(D,C) + \frac{\{O\}^t\{C\}}{\xi} \tag{4}$$

The vector $\{\mathrm{M}\}$ is related to the matrix of generalized stresses. Among other terms present in eq. (4) the matrix of flexibility $[F(D)]$ did not suffer alteration with the inclusion of corrosion, being described by eq. (5). Yet the expression of kinematic hardening starts being in the function of the corrosion eq. (6), as the increase of the resistance to the process of cracking due to the rebar, rewritten according to eq. (7). Related to the vector $\{O\}^t$ it is written for each node and it depends only on the function chosen in the literature to indicate the tax of evolution of corrosion.

$$[F(D)] = \begin{bmatrix} \frac{L_b}{3E_cI(1-d_i)} & -\frac{L_b}{6E_cI} & 0 \\ -\frac{L_b}{6E_cI} & \frac{L_b}{3E_cI(1-d_j)} & 0 \\ 0 & 0 & \frac{L_b}{AE_c} \end{bmatrix} \tag{5}$$

$$[\mathrm{H(D,C)}] = \begin{bmatrix} (1-d_i)h_i(c_i) & 0 & 0 \\ 0 & (1-d_j)h_j(c_j) & 0 \\ 0 & 0 & 0 \end{bmatrix} \tag{6}$$

$$I(D,C) = -\frac{1}{2}q(c_i)ln^2(1-d_i) - \frac{1}{2}q(c_J)ln^2(1-d_j) \tag{7}$$

With the potential already defined by eq. (4), the thermodynamic forces are written considering the corrosion, beginning with the law elasticity law, given by eq. (8), the result of the partial derivative of eq. (4) in relation to the generalized stresses $\{\mathrm{M}\}$. The yield function is linked to the thermodynamic force $\mathrm{A}^p$ generated by the partial derivative in relation to the plastic deformation, then there is eq. (9). Deriving in relation to the damage it is obtained the thermodynamic force related to the cracking $A_d$ eq. (10). And finally, the thermodynamic force associated with the corrosion $A_c$ is expressed by eq. (11).

$$\left\{\frac{\partial Gb_b}{\partial M}\right\} = [F(D)]\{\mathrm{M}\} + \{\Phi_0\} + \{\Phi^p\} = \{\Phi\} \tag{8}$$

$$\left\{\frac{\partial Gb_b}{\partial \Phi^p}\right\} = \{\mathrm{M}\} - [\mathrm{H(D,C)}]\{\Phi^p\} = \begin{Bmatrix} m_i - (1-d_i)h(c_i)\phi_i^p \\ m_j - (1-d_j)h(c_j)\phi_j^p \\ n \end{Bmatrix} = \{\mathrm{A}^p\} \tag{9}$$

$$\left\{\frac{\partial Gb_b}{\partial d}\right\} = \begin{Bmatrix} \frac{Lm_i^2}{6EI(1-d_i)^2} - q(c_i)\frac{\ln(1-d_i)}{(1-d_i)} + \frac{1}{2}h(c_i)\left(\phi_i^p\right)^2 \\ \frac{Lm_j^2}{6EI(1-d_j)^2} - q(c_j)\frac{\ln(1-d_j)}{(1-d_j)} + \frac{1}{2}h(c_j)\left(\phi_j^p\right)^2 \end{Bmatrix} = \{A_d\} \tag{10}$$

$$\left\{\frac{\partial Gb_b}{\partial cor}\right\} = -\frac{1}{2}\{\Phi^p\}^t\left[\frac{\partial H(D,C)}{\partial cor}\right]\{\Phi^p\} - \left\{\frac{\partial I}{\partial cor}\right\} + \frac{\{O\}}{\xi} = \{A_c\} \tag{11}$$

## 2.2 Evolution Laws

Since the thermodynamic introduced a new variable, it is necessary to update the evolution laws, as well as the consideration of an evolution law for the rate of corrosion. Therefore, there is in eq. (12) the damage driving moment $Y_i$ with its law of evolution in eq. (13) for a node $i$.

$$Y_i = A_{di} - \frac{1}{2}h(c_i)\left(\phi_i^p\right)^2 = \frac{Lm_i^2}{6EI(1-d_i)^2} - q(c_i)\frac{\ln(1-d_i)}{(1-d_i)} \tag{12}$$

$$\begin{cases} d_i = 0 \; if \; Y_i < R_0 \; or \; Y_i < 0 \\ d_i > 0 \; if \; Y_i = R_0 \; or \; Y_i = 0 \\ Y_i > R_0 \; or \; d_i < 0 \; impossible \end{cases} \tag{13}$$

In the same way, there is the yield function in eq. (14) followed by the evolution law of the plastic rotations in eq. (15).

$$f_i = \lfloor A_{pi} \rfloor - (1 - d_i)k_0(c_i) = \lfloor m_i - (1 - d_i)h(c_i)\phi_i^p \rfloor - (1 - d_i)k_0(c_i) \leq 0 \tag{14}$$

$$\phi_i^p = \lambda_i \frac{\partial f_i}{\partial A_{pi}}; \begin{cases} \lambda_i = 0 \; if \; f_i < 0 \\ \lambda_i > 0 \; if \; f_i = 0 \\ f_i > 0 \; impossible \end{cases} \tag{15}$$

It is important to highlight that the parameters present in the equation before shown $(h(c_i), R_0, q(c_i), k_0(c_i))$are calculated in the same way as exposed by Florez-López, Marante and Picón [7]. The divergence occurs only in the fact that now it becomes necessary to have the recalculation of those, since the degradation evolves and consequently the values of cracking moments (Mr), plastic (Mp) e ultimate (Mp) suffer penalizations.

Differently from the above laws, the law of corrosion evolution eq. (16) needs time dependency (BRANT [8]). It is clear in the below expression the composition of three parcels of different origins, the first one comes from the empirical laws $(O_i)$, followed by the term linked to the process of concrete cracking and, lastly, the parcel related to the process of the plasticity of rebars.

$$c_i = \xi A_{ci} = O_i + \xi \left( ln^2(1 - d_i)\frac{\partial q}{\partial c_i} - \phi_p^2(1 - d_i)\frac{\partial h}{\partial c_i} \right) \tag{16}$$

# 3 Experimental Procedure

## 3.1 Beam Design

The beams dimensions were adjusted based on the limitations imposed by the realization of the tests. Therefore, it was worked with a slender section (7x7 cm²) and a low tax of rebar (1 $\phi$ 6,3 mm), as due to the risk of the equipment degradation and to the test being of long duration (over 100 days), it became inviable to work with mechanical actuators, so the application of dead load was used.

To represent the beam-to-column interaction of a conventional structure, the elements show larger transversal section in the center Fig. 2, besides that, in an intentional way, remainders of the rebar were left in the extremities of the beam, in order to allow for the measurement of the corrosion potential ($E_{corr}$) to evaluate qualitatively the probability of corrosion of the rebar during the tests of long duration.

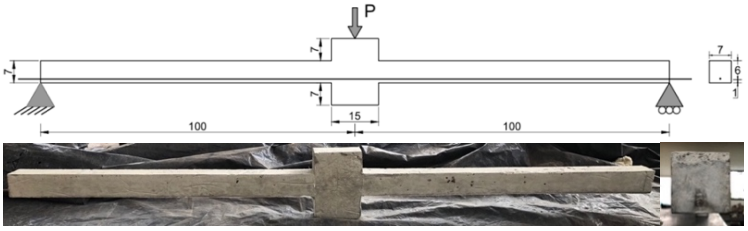


Figure 2. Beams projected and finalized (dimensions in cm).

The concrete mix used was 1 : 3,17 : 3,71 : 0,65, with cement CP V, natural fine sand and gravel 1. Furthermore, spacers adapted to guarantee 1cm of covering in the inferior part of the beam and centralized in the laterals were used, so that the rebars have little covering in the inferior face, easing the penetration by chloride.

Besides the molding of 7 beams, 10 cylindrical specimen proof (10x20cm) were prepared, aiming the characterization of the used concrete by the compressive strength test NBR 5739 (ABNT [10]) and static modulus of elasticity NBR 8522 (ABNT [11]), as well as for a first idea of how the solution of NaCl would behave when entering the beams there was a capillary absorption test NBR 9779 (ABNT [12]). Also, on the concreting day, a test was done to determine the workability of the concrete according to the NBR NM 67 (ABNT [13]). The obtained results are shown on Tab. 1.

Table 1. Results of characterization.

| State | Test | | Age [days] | Results |
|---|---|---|---|---|
| Fresh | Slump | | 0 | 6,5 cm |
| Hardened | Compressive Strength | | 28 | 42,58 MPa |
| Hardened | Static Modulus of Elasticity | | 28 | 43,33 GPa |
| Hardened | Absorption per Capillarity | % Absorption | 84 | 0,67 % |
| | | Height of Assumption | 84 | 3,95 cm |

### 3.2 Test of Long Duration

This stage demanded a long period of time (>100 days) and it was necessary a total of 6 beams for it, divided into 3 pairs in simultaneous use, where each pair received a different value of loading, besides its self-weight. Therefore, there are only 3 beams with load (reference beams) and the other 3 beams with beyond the sprinkling load of NaCl to accelerate the corrosive process.

The loading values (b1=41,14Kgf; cb1=41,15Kgf; b2=69,53Kgf; cb2=69,55Kgf; b3=113,68Kgf; cb3=113,54Kgf, each letter c shows "with presence of NaCl") were previously determined using the results of the mono-sign test, which consisted in the application and successive removal of the load. About the solution NaCl, a concentration of 3,5% was used, which was applied through a sprayer in the inferior part of the beam, which has a lower covering, easing the access of chlorides to the rebar. Furthermore, 3 beams with the process of corrosion acceleration were wrapped with geotextile membrane so that the period of humidity was increased, so there would be more symmetrical stages of wetting and drying of the beams. The process of sprinkling was realized 3 times a week.

The methodology of this test was developed so to enable the comparison between each behavior of the beams in the corrosive process, therefore, during this stage, the displacement of the beams (with and without corrosion) was collected and also the corrosion potential $E_{corr}$, which allows correlating to the probability of existing corrosion in the rebar. For the quantification of damage in the 6 beams, the process of unloading the beams was done, similar to the process done in the mono-sign test, however, here it was done only one unload and subsequent load with no increase in its value. At the beginning of the beam loading, they had 95 days after the molding, but to facilitate the understanding of the methodology, the beginning of the load was considered day 0. So, the determination of $E_{corr}$ was done on days 46, 68, 81 and 95 with de later determination of damage.

## 4 Results

### 4.1 Test of Long Duration

According to ASTM C876 [14] measurements of more electronegative than -350mV show a superior probability of 90% of being under corrosion, so, analyzing the graphics in Fig. 4 it is observed that only in bc1 on day 46 there was a data which value was inferior, supporting the following analysis. It is important to emphasize that the measures were taken in 6 different lateral spots of the beam, and in Fig. 3 there are only 3 spots indicated (0, 0,43m and 0,87m in horizontal, from the left to the center of the beam) on the 4 ages of the measurements.

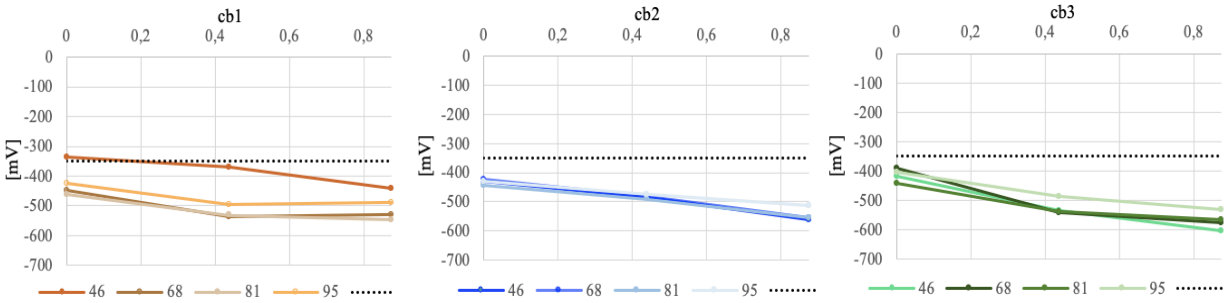


Figure 3. Measures of corrosion potential $E_{corr}$.

Based on the model detailed on item 2, and considering in the theoretical model the effects of the fluency that show along time through the coefficient calculated from the exposed in NBR 6118 (ABNT [15]) it was possible to calculate the displacement of the beams under the corrosive effect and compare them to the data experimentally collected Fig. 4. It is important to mention that the NaCl application started on the seventeenth day. It is observed that the numeric simulation presents compatibility with the results from the experiment, however, the humidity in the beams from the experiment (due to the sprinkling of the solution NaCl) may affect directly in the behavior of the fluency (decreasing it) as shown by Carbonari Santo and Toralles-Carbonari [16].

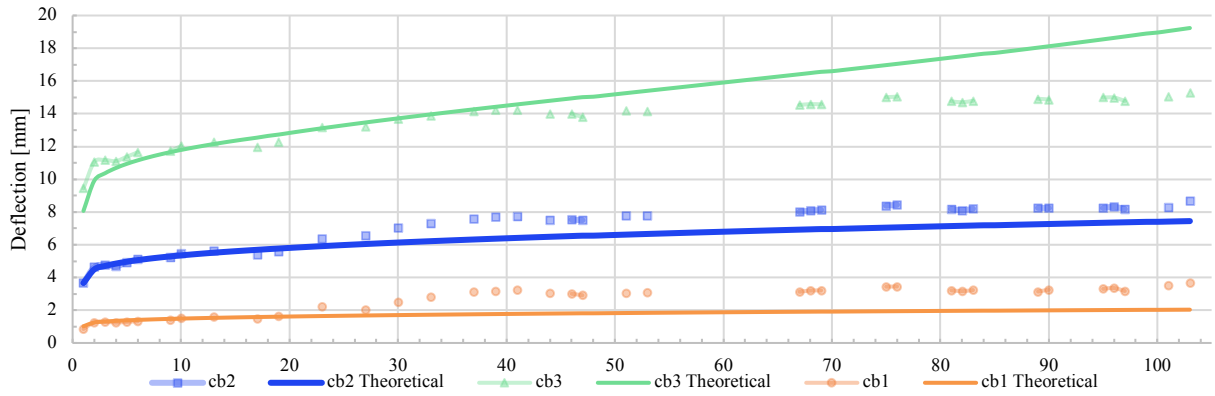


Figure 4. Deflection of beams with corrosion along time [days].

With the experimental data, it was worked on the numeric simulations. Thus, it was verified the evolution of the damage and the plastic rotation (Fig. 5), it is observed that the corrosion effect in the damage and the plastic rotation is more notorious for cb3 given it is the one which has the largest loading value.

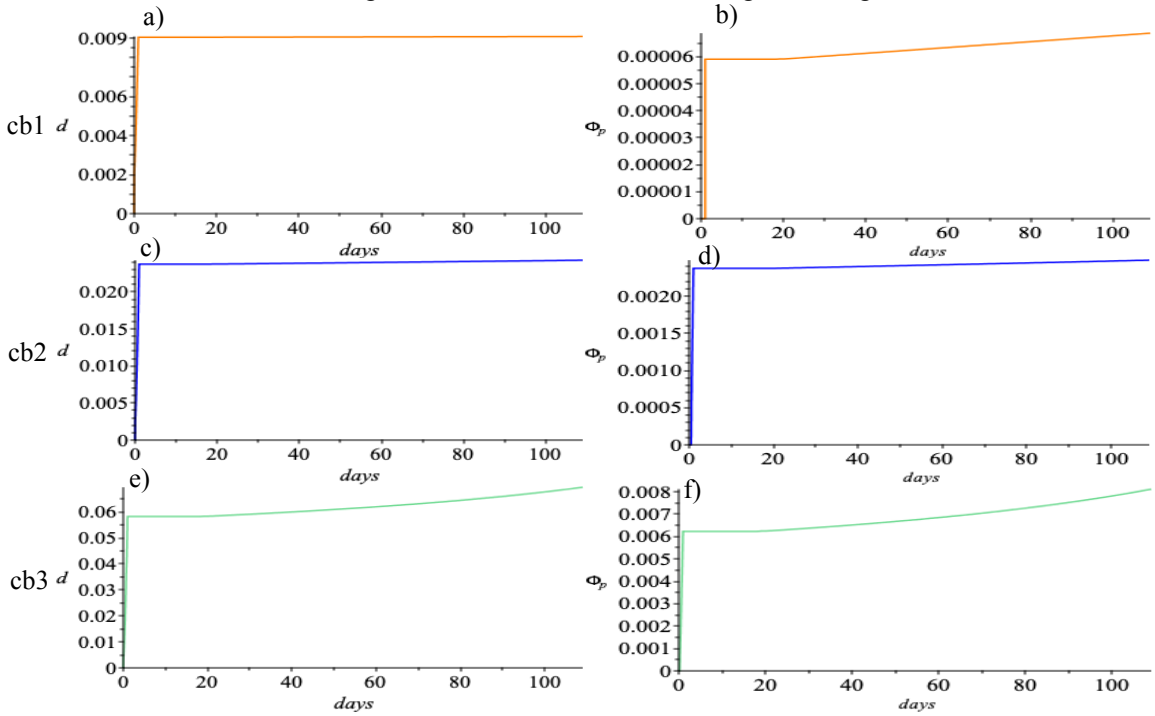


Figure 5. Variation of Damage (a, c, e) and Plastic Rotation (b, d, f) along time [days].

At last, analyzing the graphics of Fig. 6 it is possible to observe that the moments (plastic and ultimate) are penalized as long as the corrosion evolves as mentioned before, and again it is noted that these effects are proportional to the applied load.

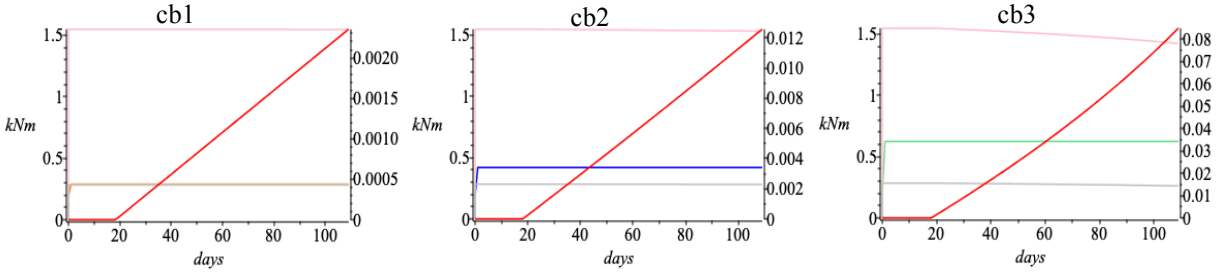


Figure 6. Variation of the Plastic Moment (grey), Ultimate Moment (pink), Currently Moment (orange "cb1", blue "cb2" and green "cb3") and corrosion (red) along time [days].

# 5 Conclusions

Through the results presented above it may be inferred:

All of the three beams submitted to the process of NaCl sprinkling presented a greater than 90% probability of being under effects of corrosion and yet, the largest values of potential corrosive detected were in the central area of the beam, where the bending moment has its maximum value and consequently also has the largest damage.

It was observed that the evolution of the damage and plastic rotation, variables defined by Lumped Damage Mechanics started to increase as there was a presence of corrosion, variable which was added by the Thermodynamics of Frames and also with the increase of these mechanical variables there was interference in the corrosion rate.

The method developed to replicate the spontaneous corrosion was effective, and it also allowed the comparison with the results of the numeric simulation of the corrosion-cracking coupling. However, it is important to highlight that it is a precursor study and, to obtain more representativeness it is necessary to elaborate a larger number of experiments. Furthermore, the possession of equipment that allows the monitoring of the corrosion intensity in the beams in a lab would facilitate the monitoring of the corrosive process.

**Authorship statement.** The authors hereby confirm that they are the solely liable persons responsible for the authorship of this work, and that all material that has been herein included as part of the present paper is either the property (and authorship) of the authors or has the permission of the owners to be included here.

# References

[1] R. C. Carvalho and J. R. D. F. Filho. Cálculo e Detalhamento de Estruturas Usuais de Concreto Armado. 3a. ed. São Carlos: EdUFSCar: [s.n.], 2007.

[2] E. Kearsley and A. Joyce. Effect of corrosion products on bond strength and flexural behavior of reinforced concrete slabs. Journal of the South African Institution of Civil Engineering., Pretoria, v. 56, n. 2, p. 21-29, August 2014.

[3] J. P. Broomfield. Corrosion of Steel in Concrete: Understanding, investigation and repair. 2. ed. Nova York: Taylor & Francis, 2006.

[4] A. Kivell, A. Palermo and A Scott. Effects of Bond Deterioration due to Corrosion in Reinforced Concrete. PCCE. Building an Earthquake-Resilient Society, Auckland, April 2011. p. 14-16.

[5] K. O. Coelho. Modelos numéricos aplicados à modelagem probabilística da degradação mecânica do concreto e corrosão de armaduras. São Carlos: USP: [s.n.], 2017.

[6] R. R. Dahmer. Modelos para análise de estruturas submetidas a solicitações químico-mecânicas. Monografia (Graduação em Engenharia Civil de Infraestrutura) - Universidade Federal da Integração Latino-Americana. Foz do Iguaçu.: [s.n.], 2018.

[7] J. Florez-López, M. E. Marante and R. Picón. Fracture and Damage Mechanics for Structural Engineering of Frames: State-of-the-Art Industrial Applications. [S.l.]: IGI Global, 2015.

[8] C. A. C. Brant. Formulação termodinâmica do acoplamento corrosão-fissuração em estruturas de concreto armado. Dissertação (Mestrado em Engenharia Civil) - Universidade Federal da Integração Latino-Americana. Foz do Iguaçu.: [s.n.], 2019.

[9] D. V. Val and R. E. Melchers "Reliability of Deteriorating RC Slab Bridges". *Journal of Structural Engineering*, pp. 1638–1644, 1997.

[10] ABNT. NBR 5739: Concreto - Ensaio de compressão de corpos de prova cilíndrico. Rio de Janeiro: [s.n.], 2018.

[11] ABNT. NBR 8522: Concreto - Determinação dos módulos estáticos de elasticidade e de deformação à compressão. Rio de Janeiro: [s.n.], 2017.

[12] ABNT. NBR 9779: Argamassa e concreto endurecidos - Determinação da absorção de água por capilaridade. Rio de Janeiro: [s.n.], 2013.

[13] ABNT. NBR NM 67: Concreto - Determinação da consistência pelo abatimento do tronco de cone. Rio de Janeiro: [s.n.], 1998.

[14] ASTM C876. Standard Test Method for Corrosion Potentials of Uncoated Reinforcing Steel in Concrete. West Conshohocken (EUA), 2015.

[15] ABNT. NBR 6118: Projeto de estruturas de concreto - Procedimento. Rio de Janeiro: [s.n.], 2014.

[16] G. Carbonari, A. C. Santos and B. M. Toralles-Carbonari. Impacto estrutural do tipo de selagem externa nas deformações fluência de vigas de concreto armado. XXXI jornadas Sud-Americanas de Ingeniería Estructural. Anais...Mendoza (ARG): 2004.